AJNR

Atrial diverticula in severe hydrocephalus.

T P Naidich, D G McLone, Y S Hahn and J Hanaway

AJNR Am J Neuroradiol 1982, 3 (3) 257-266
http://www.ajnr.org/content/3/3/257

Atrial Diverticula in Severe Hydrocephalus

Thomas P. Naidich[1]
David G. McLone[2]
Yoon S. Hahn[2]
Joseph Hanaway[3]

Massive ventricular dilatation causes stretching and dehiscence of the fornix with formation of unilateral or bilateral pial pulsion diverticula of the inferior medial wall of the atrium. Enlargement of the pial pouch creates a dramatic subarachnoid cyst that may herniate downward through the incisura into the lateral mesencephalic, precentral cerebellar, and superior vermian cisterns where it displaces the brain stem, vermis, and fourth ventricle. Lateral ventricular diverticula may be identified and distinguished from the dilated fourth ventricle and dilated suprapineal recess, with which they are so commonly confused, when all of the following signs are apparent on computed tomography (CT): (1) marked unilateral or bilateral atrial dilatation; (2) focal dehiscence of the medial atrial wall; (3) ipsilateral shortening of the tentorial band in axial section; (4) focal defect in the tentorial band in coronal section; (5) draping of the medial atrial wall over the free margin of tentorium, with continuity of cerebrospinal fluid density around the edge of tentorium in axial and/or coronal sections; (6) bowing of the crus (or crura) of fornix; (7) separation of fornix from splenium, with visualization of the hernia ostium; (8) asymmetrical position of the choroid plexi, which attach to and define the lateral borders of the fornices; (9) contralateral displacement of the internal cerebral veins; and (10) septa separating diverticulum from third ventricle.

Proper surgical management of the patient with massive hydrocephalus and a midline, incisural, cerebrospinal fluid (CSF)-density "cyst" requires accurate preoperative identification of the nature of the "cyst" and its relation to the ventricular system. Primary arachnoid and ependymal cysts, which *cause* hydrocephalus, may be treated by extirpation or direct shunting of the cyst with consequent relief of hydrocephalus. Focal ventricular dilatations that *result* from hydrocephalus are treated most effectively by simple shunting of the lateral ventricles. Initial difficulty in differentiating among primary arachnoid cysts, enlargement of the suprapineal recess of the third ventricle, pulsion diverticulum of the medial atrial wall, and upward bulging of the dilated fourth ventricle led to review of the relevant anatomy and pathology and elaboration of criteria for accurate computed tomographic (CT) diagnosis of the pulsion diverticulum of the medial wall of the atrium.

Materials and Methods

Serial CT scans of 300 pediatric and adult patients with ventricular dilatation were reviewed to select 60 patients satisfying the Meese et al. [1] criteria for extreme hydrocephalus. Patients believed to have atrophy on the basis of clinical or CT criteria were rigorously excluded. In 10 cases, where patient benefit justified the risk, CT diagnoses of atrial diverticula, arachnoid cyst, etc. were confirmed by metrizamide CT ventriculography (MCTV), metrizamide CT cisternography (MCTC), or surgical exploration [2–6].

Anatomic and Pathologic Basis for CT Signs

The medial wall of atrium is formed by the splenium above and behind, the symmetric

Received June 26, 1981; accepted after revision January 25, 1982.

Presented at the annual interim meeting of the American Association of Neurological Sciences, Section of Pediatric Neurological Surgery, New York, December 1980, and at the annual meeting of the American Society of Neuroradiology, Chicago, April 1981.

[1] Department of Radiology, Children's Memorial Hospital and Northwestern University Medical School, Chicago, IL 60614. Address reprint requests to T. P. Naidich, Children's Memorial Hospital, 2300 Children's Plaza, Chicago, IL 60614.

[2] Department of Neurological Surgery, Children's Memorial Hospital and Northwestern University Medical School, Chicago, IL 60614.

[3] Department of Neurology, Incarnate Word Hospital, St. Louis, MO 63104.

AJNR 3:257–266, May/June 1982
0195-6108/82/0303-0257 $00.00

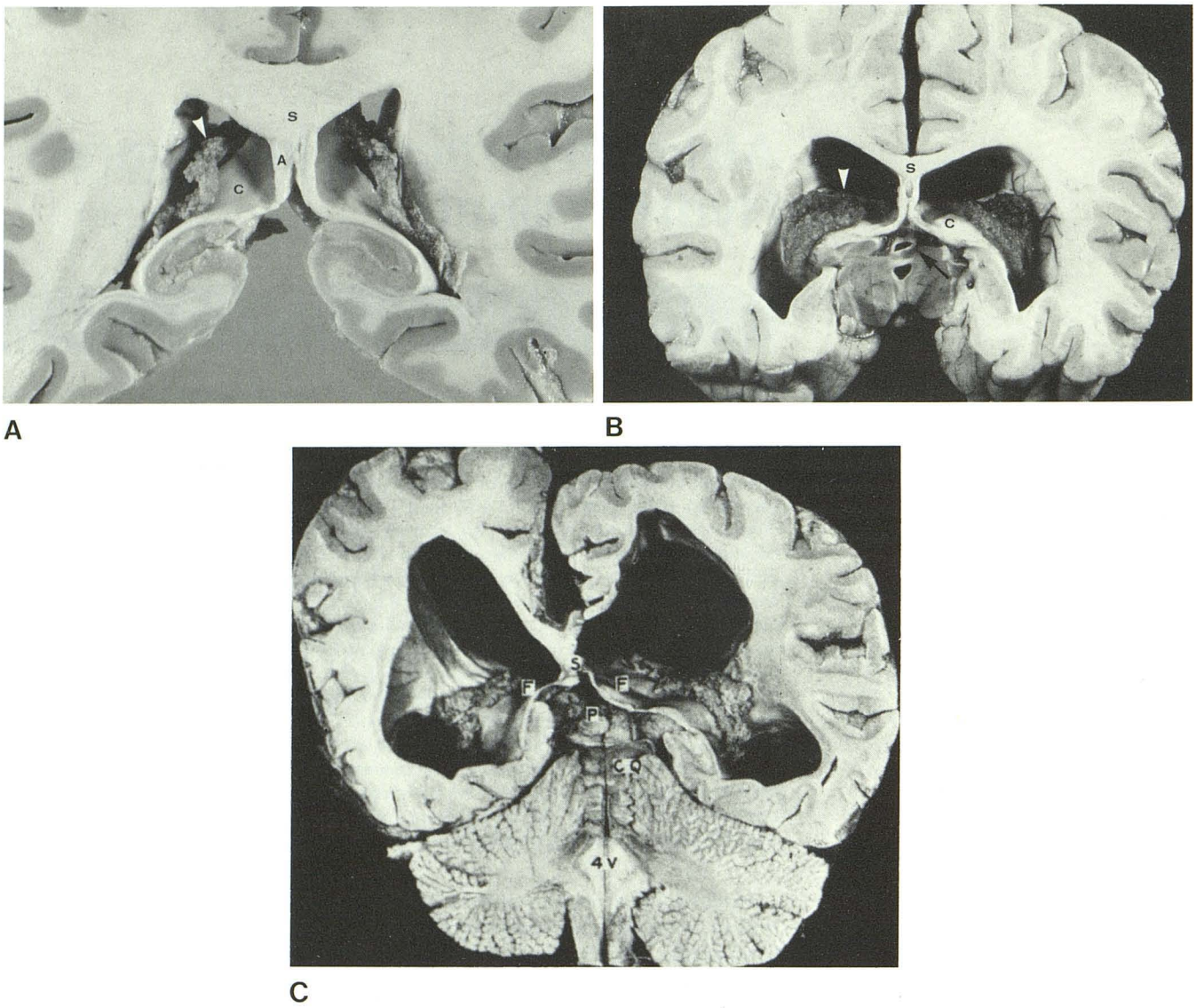

Fig. 1.—Coronal sections. **A,** Through atria of normal brain. Medial atrial wall formed by splenium of corpus callosum (S) above, symmetrical crura of fornices (C) inferiorly, and intervening alvei (A) of hippocampus. Choroid plexi (*arrowhead*) enter ventricle along lateral edges of fornix and mark its lateral edges. Distance between alveus (A) and choroid tuft indicates width of fornix and position of lateral edge. **B,** Through atria of moderately hydrocephalic brain. Corpus callosum (S) thinned and elevated. Alvei stretched. Crura of fornix (C), thinned, depressed, and displaced medially, are hollowed out and now overhang posterior third ventricle and incisura. Lateral edges of fornices and associated choroid plexi (*arrowhead*) displaced anterolaterally. Straight sinus (*arrow*) above aqueduct. **C,** Through atria of severely hydrocephalic brain. Splenium (S) is very thinned. Extremely attenuated alvei and crura of fornices (F) form hollowed-out alveocrural sheet that overhangs pineal gland (P) and corpora quadrigemina (CQ) at incisura. 4V = fourth ventricle. (Reprinted from [8].)

crura of the fornices inferiorly, and the alvei and fimbriae of hippocampus that connect the medial edges of the crura to the undersurface of splenium (fig. 1A) [7–10]. Ependyma lines the inner aspect of the atrial wall. Very thin hippocampal gyrus and pia mater line the outer aspect of the atrial wall. The choroid plexi lie symmetrically along the lateral edges of the fornices where the tela choroidea emerges from the choroidal fissure. The positions of the choroid plexi are reliable landmarks for the lateral edges of the fornices.

With progressive hydrocephalus and progressive expansion of the atria, the splenium is thinned, elevated, and displaced posteriorly (fig. 1B) [8–11]. The crura of the fornices are depressed and thinned. The medial edges of the crura are displaced medially. The *lateral* edges of the thinned crura are displaced laterally and anteriorly. The choroid plexi that mark the lateral edges of the crura are similarly displaced laterally and anteriorly. The alvei are displaced medially and stretched between the elevated splenium and the depressed crura.

At this stage, the medial wall of atrium has been displaced medial to the free edge of the tentorium and now overhangs the incisura without support [8]. The medial atrial wall is intact and can be traced, in continuity, from the midline alvei along the thinned, *inferiorly convex* crura to the choroid plexi at the lateral edges of the crura (fig. 1B).

With greater atrial dilatation, the alveus and crus of fornix become an extremely thinned alvear-crural sheet that may be focally dimpled

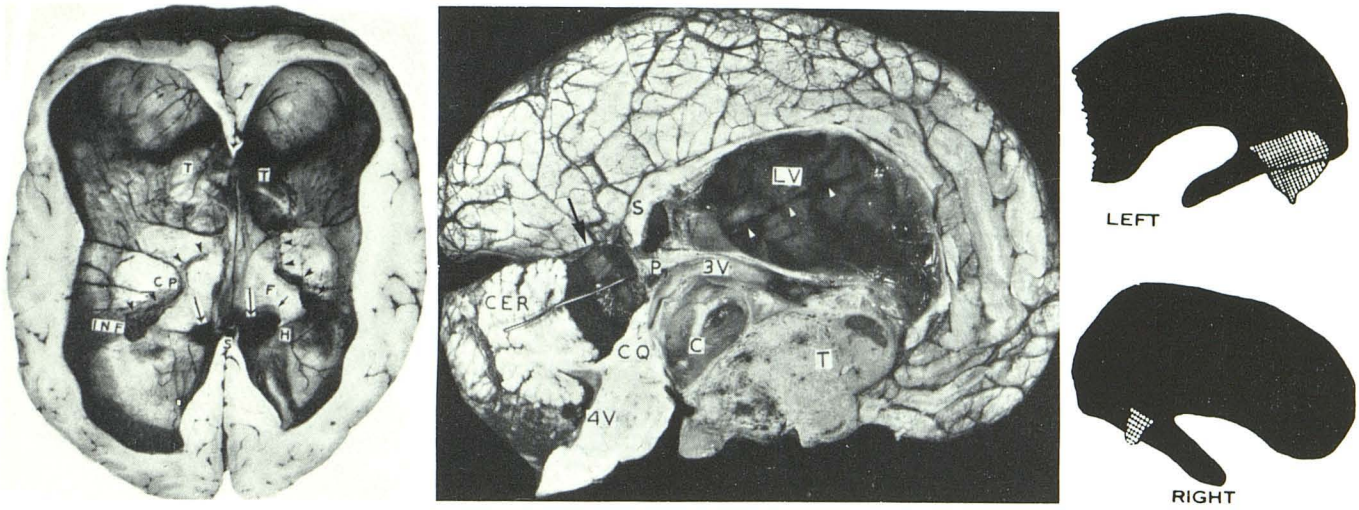

Fig. 2.—7½-year-old girl with severe hydrocephalus and bilateral, asymmetrical atrial diverticula. Hydrocephalus secondary to cystic polar spongioblastoma of hypothalamus and anterior third ventricle. **A,** Axial section through severely dilated lateral ventricles. Bilateral diverticulum ostia (*long arrows*). Ostia are delimited posteromedially by thinned, elevated, posteriorly displaced splenium (S) and delimited anterolaterally by displaced crura of fornix (F). Choroid plexi (CP, *arrowheads*) are displaced anterolaterally with lateral edges of fornix, but still mark position of fornix. Posteromedial borders of crura are now concave (*short arrow*), where they arc around hernia ostium. INF = inferior horn of ventricle, T = tumor. **B,** Lateral view of left half of brain sectioned through midline. Probe (*arrowheads*) passes from left lateral ventricle (LV) through ostium (seen in **A**) into precentral cerebellar fissure cyst (*arrow*). Infratentorial part displaces cerebellum (CER) posteroinferiorly, fourth ventricle (4V) directly inferiorly, and corpora quadrigemina (CQ) anteroinferiorly. Splenium displaced superiorly. T = tumor, C = cystic component of tumor, 3V = third ventricle. **C,** Diagrams of gas ventriculogram illustrate cross-hatched area of atrial diverticula and sites of origin from dilated lateral ventricles. (**A** and **B** reprinted from [8].)

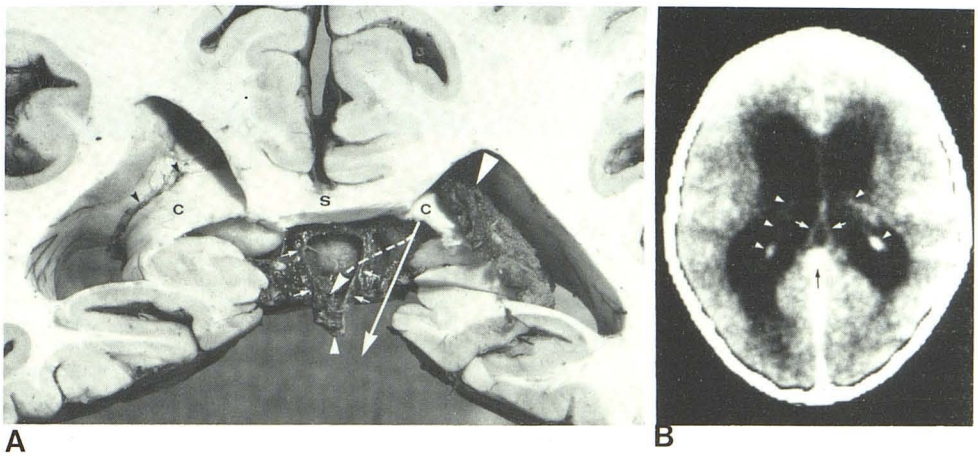

Fig. 3.—Relations among crura, choroid plexi, and internal cerebral veins. **A,** Coronal section through atria from behind, after partial resection of splenium (S). On right side, choroid plexus (*large white arrowhead*) partly overlaps crus (C) of right fornix. Resection of left choroid plexus exposes full crus (C) and origin of choroid plexus from tela choroidea at lateral edge of fornix (*black arrowheads*). Two internal cerebral veins (*short white arrows*) join to form vein of Galen (*small white arrowhead*) in midline. Unilateral atrial diverticulum that extends infratentorially would follow course of long white arrow to displace choroid plexus laterally and internal cerebral veins contralaterally, widening gap between them. Dashed sidearm of long white arrow indicates infrequent medial extension of diverticulum over internal cerebral vein into cistern of velum interpositum. **B,** Contrast-enhanced axial CT in hydrocephalic patient without pulsion diverticulum. Two internal cerebral veins (*white arrows*), vein of Galen (*black arrow*), and symmetrical glomera and bodies of choroid plexi (*arrowheads*). Distance between glomera and internal cerebral veins estimates sizes and positions of crura of fornices.

or markedly translucent (fig. 1C) [8, 11, 12]. This sheet may be denuded of ependyma focally [11, 12]. The hippocampal gyrus is attenuated to obliteration. The pia remains intact.

Infrequently, the attenuated alvear-crural sheet dehisces or shears away from the splenium creating unilateral or bilateral diverticulum ostia 5–20 mm in diameter (fig. 2A) [8, 10]. These ostia are bordered by the thinned splenium posteromedially and the displaced crura anterolaterally [8–10]. The choroid plexus in such cases is displaced anterolaterally with the displaced lateral edge of fornix. The continuity of the medial atrial wall is disrupted at the dehiscences. The normal posteromedial convexity of the medial edge of the crus is now concave where it arcs around the hernia ostium.

After the ostium forms, CSF pushes through the remnant mantle

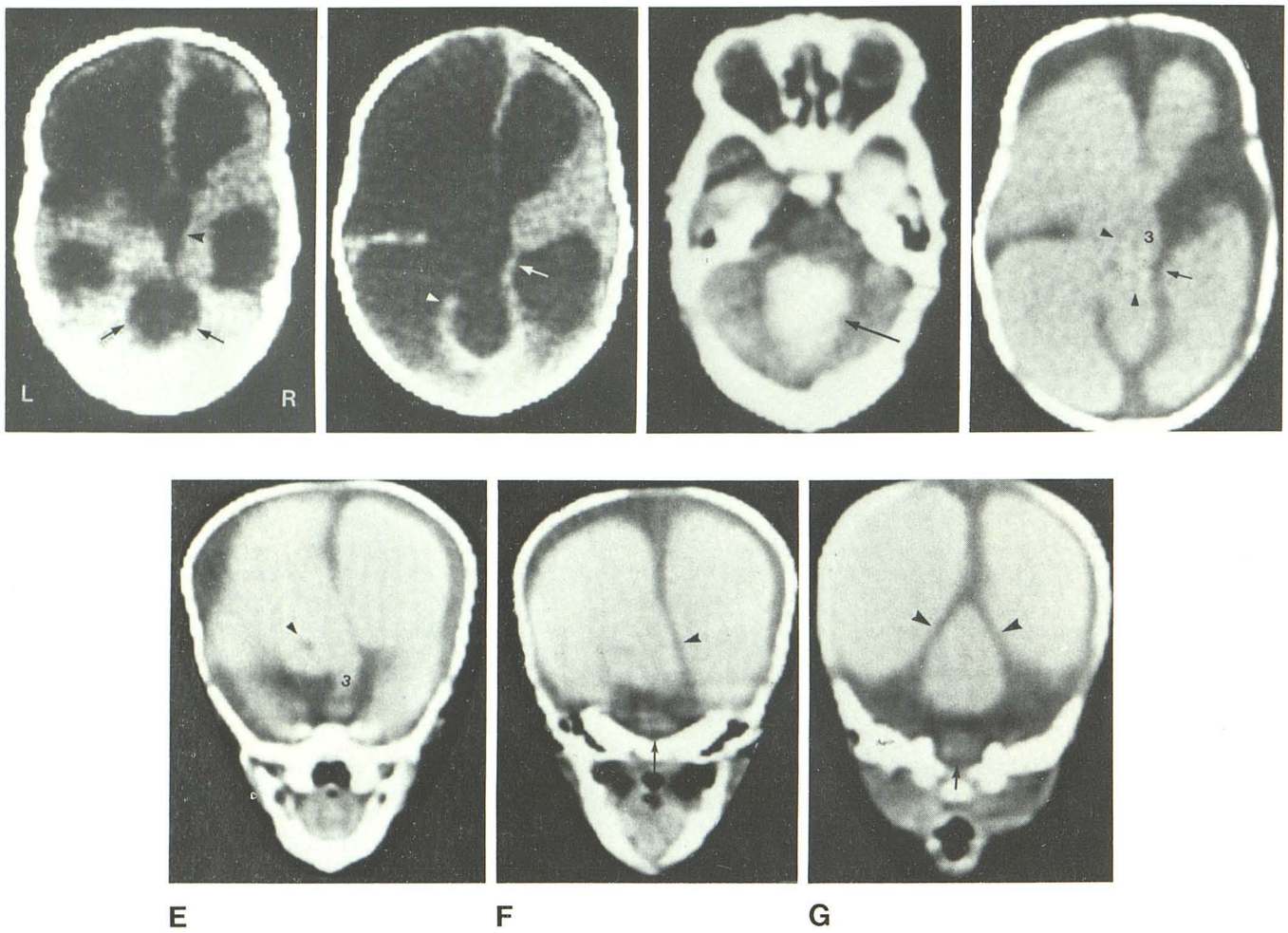

Fig. 4.—Unilateral atrial diverticulum, 2-month-old girl with congenital hydrocephalus. **A,** Noncontrast scan. Hydrocephalus with larger left lateral ventricle. Third ventricle (*arrowhead*) lies to right of midline. Large, round, midline CSF-density atrial diverticulum (*arrows*) was initially mistaken for dilated fourth ventricle. **B,** Higher contrast-enhanced scan. Asymmetrically shorter tentorial band (*arrowhead*) on side of larger ventricle. Right atrial wall (*arrow*) intact. Left atrial wall not discernible. Continuity of CSF density between dilated left atrium and midline CSF-density cyst. **C** and **D,** Axial MCTV scans displayed from below upward. Large opacified posterior fossa "cyst" (*long arrow*), rightward displacement of third ventricle (3), intact right atrial wall (*short arrow*), dehiscent left atrial wall, and continuity of opacified CSF from dilated left atrium into midline cyst. Two linear filling defects (*arrowheads*) believed to represent internal cerebral veins. **E–G,** Direct coronal MCTV from anterior to posterior. **E,** Anteriorly, diverticulum indented by internal cerebral vein (*arrowhead*). Medial part of diverticulum drapes over internal cerebral vein into cistern of velum interpositum and displaces third ventricle (3) inferiorly and rightward. **F,** At hernia ostium. Wedgelike diverticulum arises from the left medial atrial wall, extends inferomedially into posterior fossa, and displaces fourth ventricle (*arrow*) inferiorly (cf. 2C). Soft-tissue density of tentorium and cerebral mantle (*arrowhead*) seen on contralateral side is absent at level of ostium of diverticulum. **G,** Behind ostium diverticulum. Dilated atria, large midline, opacified space separated from atria by falx and tentorium (*arrowheads*), and inferiorly displaced fourth ventricle (*arrow*).

and bulges the pia inferomedially to form a pulsion diverticulum of the inferomedial atrial wall. The diverticulum protrudes into the subarachnoid space, comes into contact with the arachnoid mater, and displaces the arachnoid before it as it grows [8–10]. The pia remains intact, preventing communication between the ventricle and the subarachnoid space. With progressive enlargement, the pial diverticulum and displaced arachnoid surrounding it bulge downward through the incisura alongside and behind the midbrain to form an incisural and subtentorial cyst within the ambient and superior vermian cisterns and the precentral cerebellar fissure (fig. 2B) [8–12]. Such cysts range in size from 2 × 2 × 2 cm up to 7 × 5 × cm [10]. The cyst typically displaces the quadrigeminal plate and pineal gland anteroinferiorly, displaces the fourth ventricle directly inferiorly, displaces the anterior vermis posteroinferiorly, displaces the straight sinus and tentorium posterosuperiorly, and displaces the vein of Galen and occipital lobes anterosuperiorly (fig. 2B) [8, 10].

Gas ventriculograms in such patients document that these diverticula may be unilateral or bilateral and symmetrical or asymmetrical (fig. 2C) [8]. They usually communicate with a single lateral ventricle but may rarely communicate with both lateral ventricles [13]. Histologic examination of the cyst wall shows pia mater with tags of white matter adherent to it [10]. Ependymal lining cells have not been recognized [8, 10, 14]. Occasionally, the membrane appears hemorrhagic [14]. In the single sample analyzed, the cyst fluid was similar to CSF but with substantially higher protein content than the lateral ventricle (138 mg/dl versus 20 mg/dl), implying partial loculation [15].

Appreciation of the appearance of atrial diverticula on contrast-enhanced CT requires understanding of three additional anatomic

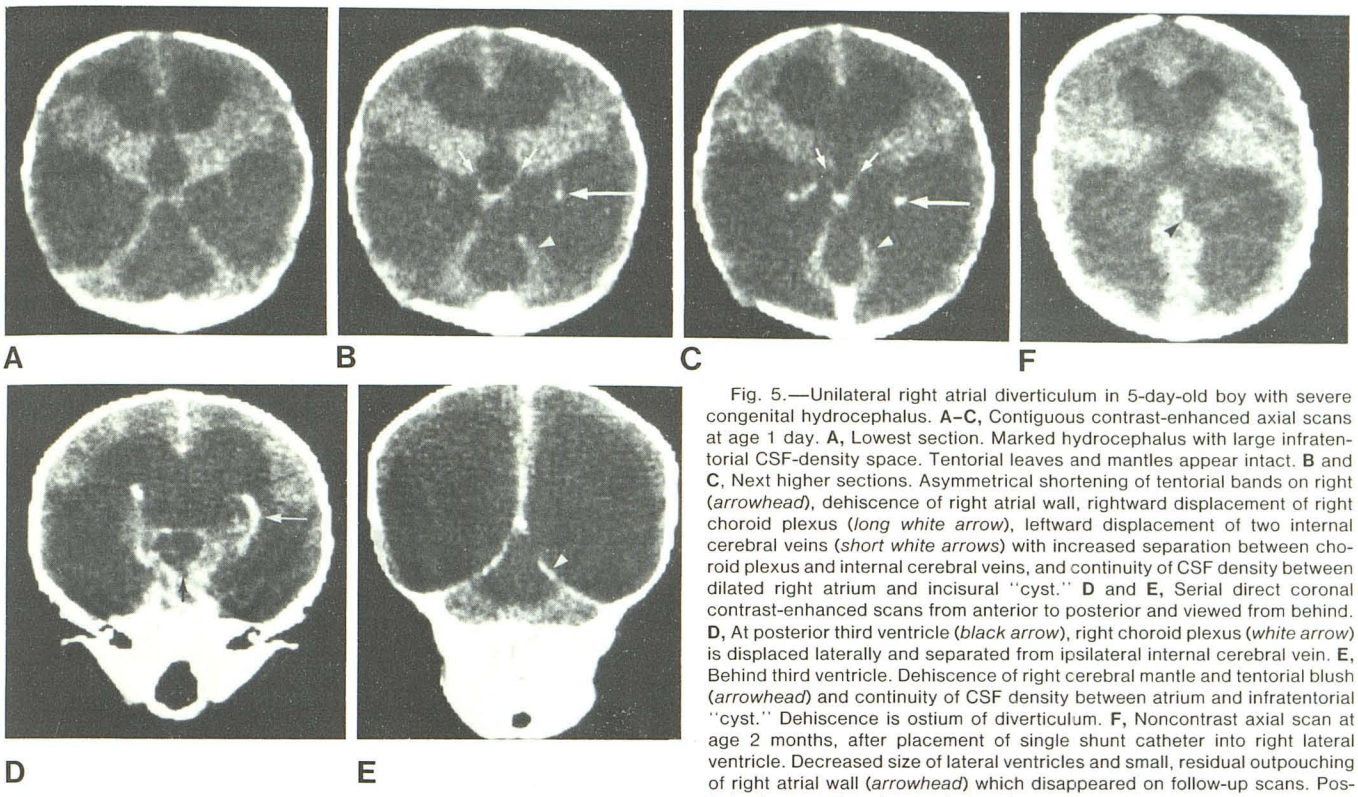

Fig. 5.—Unilateral right atrial diverticulum in 5-day-old boy with severe congenital hydrocephalus. **A–C,** Contiguous contrast-enhanced axial scans at age 1 day. **A,** Lowest section. Marked hydrocephalus with large infratentorial CSF-density space. Tentorial leaves and mantles appear intact. **B** and **C,** Next higher sections. Asymmetrical shortening of tentorial bands on right (*arrowhead*), dehiscence of right atrial wall, rightward displacement of right choroid plexus (*long white arrow*), leftward displacement of two internal cerebral veins (*short white arrows*) with increased separation between choroid plexus and internal cerebral veins, and continuity of CSF density between dilated right atrium and incisural "cyst." **D** and **E,** Serial direct coronal contrast-enhanced scans from anterior to posterior and viewed from behind. **D,** At posterior third ventricle (*black arrow*), right choroid plexus (*white arrow*) is displaced laterally and separated from ipsilateral internal cerebral vein. **E,** Behind third ventricle. Dehiscence of right cerebral mantle and tentorial blush (*arrowhead*) and continuity of CSF density between atrium and infratentorial "cyst." Dehiscence is ostium of diverticulum. **F,** Noncontrast axial scan at age 2 months, after placement of single shunt catheter into right lateral ventricle. Decreased size of lateral ventricles and small, residual outpouching of right atrial wall (*arrowhead*) which disappeared on follow-up scans. Posterior fossa cyst no longer detected.

relationships:

1. Figure 3 depicts the relation among the medial atrial wall, the choroid plexus, the internal cerebral veins, and the vein of Galen in an anatomic specimen (fig. 3A) and a contrast-enhanced CT scan (fig. 3B) [16]. Unilateral atrial diverticula that extend downward into the quadrigeminal plate cistern will displace the internal cerebral veins and the vein of Galen to the opposite side. Simultaneously, they will displace the crus of fornix *and the accompanying choroid plexus* ipsilaterally, widening the distance between the choroid plexus and the internal cerebral veins on the side of the diverticulum. Bilateral atrial diverticula will squeeze the two internal cerebral veins between them and displace the veins away from the larger diverticulum. Infrequently, medial extension to the cistern of the velum interpositum will cause the diverticulum to drape over the ipsilateral internal cerebral vein (figs. 3A, 4D, and 4E). Rarely, atrial distension may displace the ipsilateral choroid plexus asymmetrically closer to the midline despite the presence of a diverticulum ostium.

2. Contrast-enhanced CT sections through the upper tentorium near the apex of incisura depict the left and right tentorial leaves as a V-shaped blush [17]. In properly positioned, normal patients, the length and position of the two sides of the V are very symmetrical. Severe, asymmetric hydrocephalus in utero would be expected to cause greater migration and lower insertion of the tentorium on the side of the larger ventricle. The consequent tentorial asymmetry would cause corresponding asymmetry of the V blush with a shorter tentorial blush on the side of the larger ventricle and lower tentorial leaf. Conceivably, pressure deflection or pressure attenuation of the tentorial edge could also cause an asymmetrically shorter, ipsilateral tentorial blush. Severe bilateral hydrocephalus in utero would cause unusually low insertion of the tentorium with bilaterally short and stubby arms of the V.

3. On contrast-enhanced CT, the anterior ends of the tentorial bands mark the free margins of the tentorium at the level of the section [18]. The gap between the anterior ends of the tentorial bands, therefore, marks the exact site of the incisura at the level of the section. Lesions situated lateral to the tentorial bands or anterior to the anterior ends of the tentorial bands are supratentorial. Lesions situated between the tentorial bands are infratentorial and/or incisural. Therefore, on contrast-enhanced scans, any lesion that drapes over the anterior end of the tentorial band on CT is crossing through the incisura in vivo [18].

Results

Review of the numerous serial CT scans of each of the 60 patients with extreme hydrocephalus disclosed 15 (25%) with CT signs of medial atrial diverticulum (figs. 4–8). These signs include: (1) marked unilateral or bilateral atrial dilatation; (2) focal dehiscence of the medial atrial wall; (3) characteristic ipsilateral shortening of the tentorial band in axial section CT; (4) focal defect in the tentorial band in coronal section CT; (5) draping of the medial atrial wall over the free margin of tentorium, with continuity of CSF density around the edge of tentorium in axial and/or coronal section CT; (6) separation of fornix from splenium, with visualization of the hernia ostium; (7) anterolateral bowing of the crus (or crura) of fornix around the hernia ostium; (8) asymmetrical position of the choroid plexi that attach to and define the lateral borders of the fornices; (9) contralateral displacement of the internal cerebral veins; and (10) septa separat-

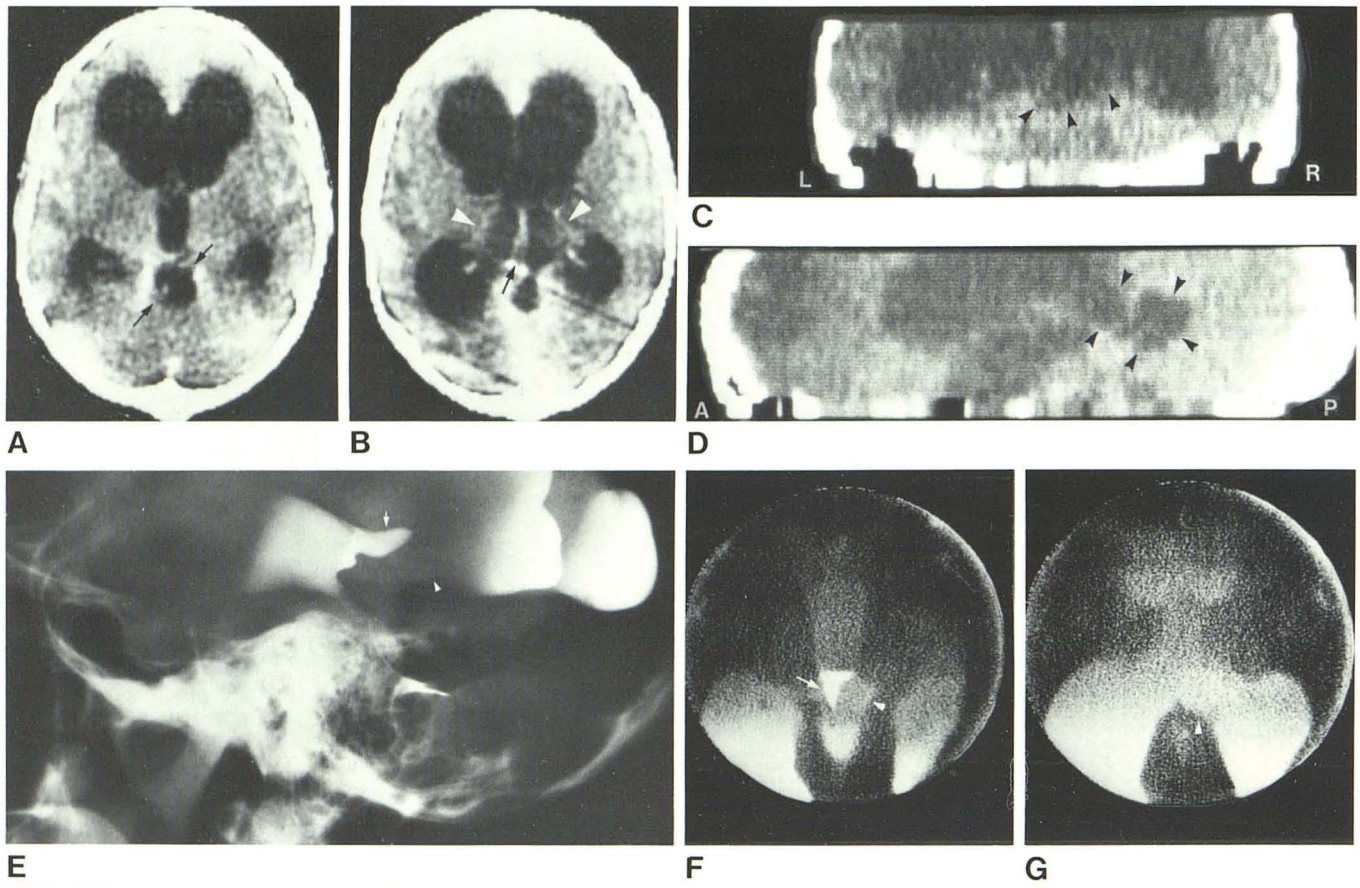

Fig. 6.—Combined suprapineal recess and lateral ventricular diverticulum, 10-year-old girl. **A,** Axial contrast-enhanced scan. Dilatation of third and lateral ventricles; midline incisural CSF-density "cyst" initially interpreted as dilated suprapineal recess. Small soft-tissue density (*arrows*) crosses this space. **B,** Next higher level. Leftward displacement of both internal cerebral veins (*arrow*) and rightward displacement of right choroid plexus (*arrowheads*). Interval between *left* choroid plexus and *left* internal cerebral vein marks width and position of left fornix. Greater interval on *right* indicates anterolateral displacement of *right* crus of fornix. Right fornix seen faintly just medial to the ipsilateral choroid plexus. Concave posteromedial border of right crus defines margin of diverticulum ostium. Continuity of CSF density through this ostium into incisural cyst (cf. 2A for shape and position of right crus and ostium). Reconstructed coronal (**C**) and sagittal (**D**) noncontrast scans confirm wedge-shaped diverticulum (*arrowheads*) of inferomedial wall of right atrium and its infratentorial extension. **E,** Lateral brow-up metrizamide ventriculogram. Small, densely opacified suprapineal recess (*arrow*) and broader, less well-defined right atrial diverticulum (*arrowhead*). Gravitational layering of hyperbaric contrast prevents complete visualization of ventricles and diverticulum. **F** and **G,** Serial 5 mm high-resolution axial scans during same metrizamide ventriculogram (displayed from bottom upward). Small outpouching of right atrial wall (*arrowhead*) leads directly inferiorly along right side of denser, displaced suprapineal recess (*arrow*) into diverticulum within quadrigeminal plate cistern. This collection flattened collicular plate. **H,** Computer-reformatted coronal MCTV, viewed from behind. Intact left atrial wall, displaced suprapineal recess (*arrow*), dehiscent right inferior medial atrial wall, and wedge-shaped right atrial diverticulum (*arrhowhead*).

ing diverticulum from third ventricle. These signs are all present in each case, but must be sought specifically by closely spaced axial and direct coronal images through the atrium and incisura, whenever the diverticulum is small.

In difficult cases, MCTV and MCTC may be used to document direct continuity between the lateral ventricle and the incisural cyst (figs. 4 and 6) [19]. The wedge-shaped density that arises at the inferomedial aspect of the atrium and extends downward and medially into the posterior fossa is characteristic of the lateral ventricular diverticulum (fig. 4). Once appreciated on MCTV, it can be recognized as a wedge-shaped CSF space on direct or reformatted coronal images obtained without metrizamide (figs. 6C and 6D).

The changes described do *not* reflect asymmetry of atrial size alone (fig. 9). Simple asymmetry may be associated with some dural deformities and midline shift but will not cause discontinuity of the atrial wall, draping of CSF density over the anterior end of the tentorial band, or wedgelike inferior extensions of CSF on coronal scans.

In the group of 15 patients with ventricular diverticula, the diverticula were bilateral in four and unilateral in 11. They were large in five cases and small in the rest. In almost every case, the diverticula regressed completely after shunting the ipsilateral lateral ventricle relieved the patient's hydrocephalus. Occasionally, a small outpouching of the medial atrial wall indicated the site of a once-large "cyst"

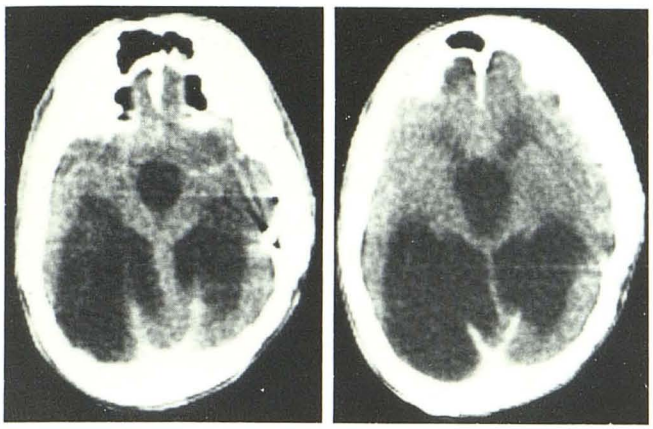

Fig. 7.—Bilateral atrial diverticula. Contrast-enhanced axial scans in 15-year-old boy. Stubby and asymmetrical tentorial bands. Medial atrial walls drape over free edge of tentorium bilaterally. Pial investments compressed to soft-tissue septum in midline.

Fig. 9.—Markedly asymmetric atrial dilatation with no diverticulum. Absence of any CT signs described for diagnosis of atrial diverticulum indicates that signs are specific for diverticulum rather than simple atrial asymmetry.

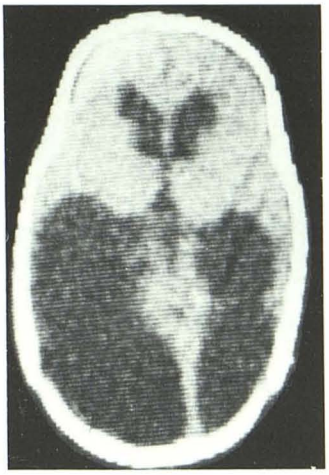

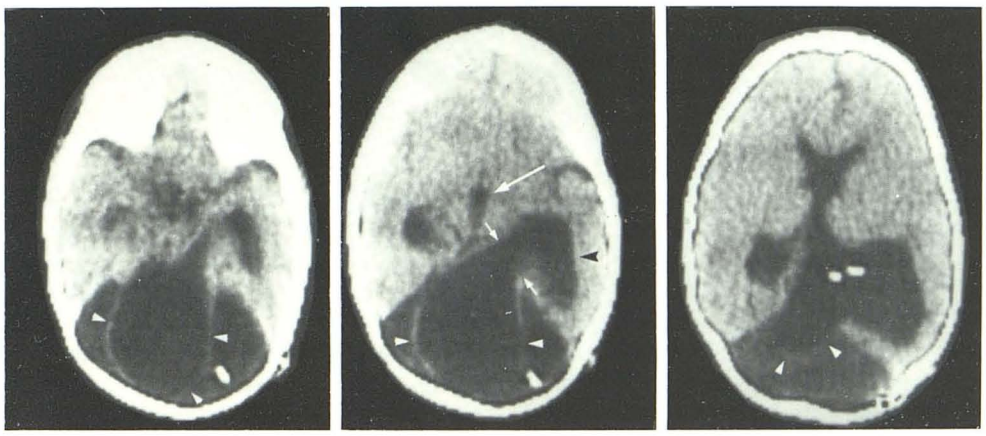

Fig. 8.—Atrial diverticulum invaginates into Dandy-Walker cyst in 2-year-old boy with Dandy-Walker malformation initially shunted directly into cyst. Poor drainage of lateral ventricles caused dilatation of right atrium and formation of right atrial diverticulum, which descended into posterior fossa, necessitating shunting of right lateral ventricle. **A** and **B**, Serial noncontrast scans from below upward. Posterior fossa shunt, dilated right atrium (*black arrowhead*), dehiscent medial wall (*short arrows*), and leftward displacement of third ventricle (*long arrow*). Pial sac (*white arrowheads*) delimits atrial diverticulum, which invaginates into, but remains isolated from, Dandy-Walker cyst. Pneumography confirmed CT interpretation. **C,** Diverticulum (*arrowheads*) persisted after shunt decompression of dilated right atrium. (Case courtesy of Douglas Yock, Metropolitan Medical Center, Minneapolis, Minn.)

(fig. 5F). Rare diverticula persist after supposedly successful shunt decompression of the lateral ventricle (fig. 8C).

Because MCTV could not be justified in many of these cases, the accuracy of these diagnoses and, therefore, the true incidence of atrial diverticulum remain presumptive. Every effort was made to count only "clear-cut" examples of diverticulum, so even the surprisingly high figure of 25% is believed to be a conservative estimate of the incidence of such diverticula in patients with *massive* hydrocephalus.

In this series, no patient with atrial diverticulum was found to have an obstructing neoplasm, although early reports of atrial diverticula emphasized the association of such diverticula with hydrocephalus caused by brain stem gliomas, hypothalamic gliomas, third ventricular epidermoidomas, and other tumors [8, 9, 12, 13, 20]. Granular ependymitis [14], aqueductal gliosis [10, 12], and external obstructive hydrocephalus [10, 15] were considered infrequent causes of atrial diverticula.

Differential Diagnosis

The atrial diverticulum has been confused with: (1) the dilated fourth ventricle associated with outlet fourth ventricular obstruction or isolated fourth ventricle [21, 22], (2) the dilated suprapineal recess of an aqueductal stenosis, and (3) the primary arachnoid cyst of the incisura:

The midline incisural "cyst" caused by upward bulging of a dilated fourth ventricle, or Dandy-Walker cyst, may be

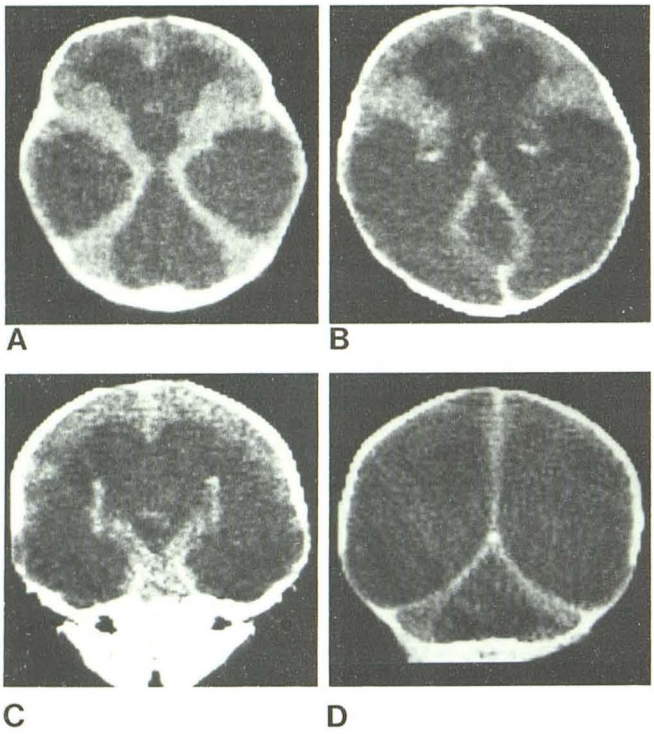

Fig. 10.—Large fourth ventricle in newborn boy with obstruction at exit foramina of fourth ventricle. **A** and **B**, Serial axial contrast-enhanced scans. Tentorial bands, atrial wall, and choroid plexi intact and symmetrical bilaterally. Internal cerebral veins (not shown) were not displaced. **C** and **D**, Serial direct coronal contrast-enhanced scans. Intact atrial walls, intact tentorial bands, and symmetrical choroid plexi.

recognized by the demonstration of symmetry and integrity of the tentorial bands and atrial walls, symmetrical choroid plexi and internal cerebral veins, and lack of direct continuity between cyst and atrium (fig. 10). MCTV will confirm absence of direct communication between "cyst" and lateral ventricle. If the fourth ventricle or Dandy-Walker cyst communicates normally through the aqueduct of Sylvius with the lateral and third ventricles, the posterior fossa "cyst" will usually persist after shunting, but will become reduced in size and more nearly normal in shape. If the fourth ventricle does not communicate with the lateral and third ventricles, it will persist unchanged or bulge further upward after shunting of the lateral ventricles. Such isolated fourth ventricles may be difficult to distinguish from primary arachnoid cysts. A round or pearlike shape, absence of a separate, inferiorly displaced fourth ventricle, and extension of the "cyst" into the region normally occupied by the fourth ventricle favor a diagnosis of a large fourth ventricle [21, 22].

The midline dilated suprapineal recess may be identified accurately by demonstration of continuity of CSF-density between the diverticulum and third ventricle; integrity and symmetry of the medial atrial walls with distinct septa separating atria from the midline recess; and symmetrical choroid plexi (fig. 11). Symmetrical internal cerebral veins may also be seen. When an atrial diverticulum coexists with a slightly prominent suprapineal recess, each component may be recognized independently (fig. 6).

Primary arachnoid cysts of the incisura may be distinguished by the intact walls separating them from the surrounding atria, third ventricle, and fourth ventricle. MCTV, MCTC, and/or air CT cisternography will show no direct, rapid communication of the cyst with the ventricles or cisterns. However, the cyst density may increase moderately over 8–12 hr from slow passage of metrizamide across the cyst wall [6, 23]. To our knowledge, complete loculation of an atrial diverticulum, a potential diagnostic pitfall, has not been reported as yet.

Unusual arachnoid cysts of the posterior temporal fossa may extend infratentorially and mimic many of the signs of the atrial diverticulum (fig. 12). However, detection of the intact medial atrial wall and recognition that the lateral ventricles are separate, compressed, and displaced will usually indicate the correct diagnosis. Cyst puncture with metrizamide CT cystography will then confirm that the lesion is isolated from the ventricle and cisterns. Metrizamide CT cisternography may also confirm the diagnosis [19].

Cystic neoplasms of the deep structures, for example, cystic thalamic astrocytoma, may also mimic the appearance of the lateral atrial diverticulum. Detection of the tumor mass distinguishes these lesions from the atrial diverticulum in most cases.

Discussion

Pulsion diverticula of the atria of the lateral ventricles were first reported by Penfield [13] in 1929, although Turnbull recognized the essential nature of the condition in 1923 (cited in [11, 12]). The anatomic derangements responsible for the diverticulum were described by Sweet [9] (case 2) in 1940. This description was amplified and correlated with the pneumographic appearance of these lesions in 1942 in two independent reports by Childe and McNaughton [8] and by Dyke [20]. Pennybacker and Russell [12] (1943) described the first surgical approach to these lesions, and MacFarlane and Falconer [10] (1947) described the first successful treatment of hydrocephalus by resection of the pial and arachnoidal wall of the diverticulum to establish free communication between the atrium and the subarachnoid space at the cisterna ambiens. Additional reports by Perryman and Pendergrass [24] and others have been summarized by Kruyff [25].

To our knowledge, the first angiographic description of these diverticula was by Alonso et al. [26] in 1979. Naidich et al. [17] (1977) published the first CT image of a lateral ventricular diverticulum.

The nomenclature of this lesion has been extremely confusing. The same entity has been termed arachnoid cyst of the cisterna ambiens (Noetzel, cited in [24]), spontaneous ventriculostomy [26], cerebral ventriculostium [9], spontaneous ventricular rupture [12, 14], and ventricular diverticulum [8, 15, 20, 26]. In part, this confusion represented the difficulty of distinguishing diverticulum formation from true rupture by pneumography and oily contrast ventriculography. Since the relations of tissue planes and spaces may

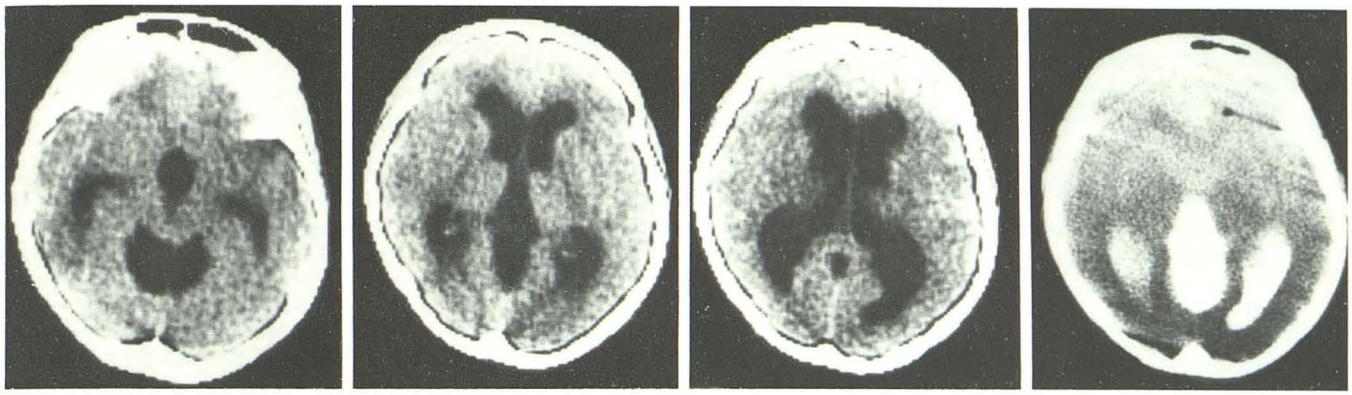

A B C D

Fig. 11.—Infratentorial herniation of suprapineal recess, 44-year-old woman. **A–C,** Noncontrast scans. Superior vermian and quadrigeminal plate cisterns occupied by CSF-density "cyst" directly continuous with third ventricle and well separated from mildly dilated atria. Atrial walls and choroid plexi are symmetrical. **D,** Metrizamide ventriculogram. Continuity of opacified CSF from third ventricle to incisural "cyst." (Case courtesy of Norman Leeds and Robert D. Zimmerman, Montefiore Hospital and Medical Center, Bronx, N.Y.)

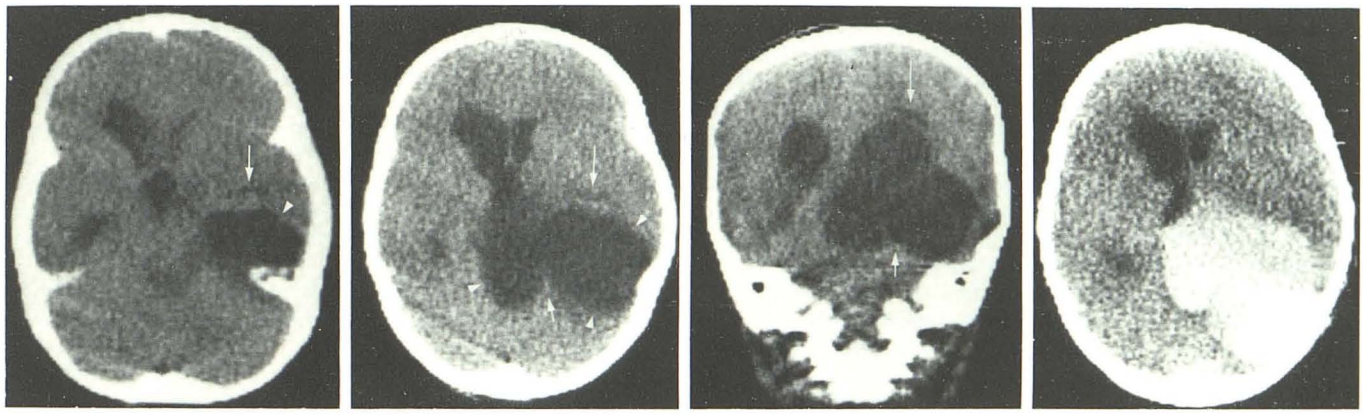

A B C D

Fig. 12.—Posterior temporal arachnoid cyst with incisural extension, 4-year-old boy. **A** and **B,** Axial noncontrast scans. Ovoid posterior temporal CSF-density cyst (*arrowheads*) compresses right lateral ventricle and displaces temporal horn (*long arrows*) anteriorly. Cyst is notched posteriorly (*short white arrow*) where it drapes over free edge of right tentorial leaf. **C,** Direct coronal noncontrast scan, viewed from behind. Compression and elevation of right atrium (*long arrow*) by large posterior temporal and incisural cyst. Notch in cyst wall at free edge of tentorium (*short arrow*). **D,** Axial metrizamide CT cystogram corresponds to **B**. CSF-density space is cyst that communicates with neither ventricular system nor subarachnoid cisterns.

now be established by CT and MCTV, we urge that the pial-lined cystic space that is walled off from the subarachnoid space and that communicates only with the ventricle be designated "ventricular diverticulum." This designation should be modified to indicate the ventricle of origin, for example, lateral (or third) ventricular diverticulum. The term *ventriculocisternostomy* should be used to designate free communication between the ventricle and the entire subarachnoid space [27–29]. This term may also be modified to indicate the ventricle of origin and whether such communication arose spontaneously or postoperatively. Rare ventriculosubdural communications [11, 14], ventriculosubgaleal communications [30], and external fistulae [11, 31] may be described by similar designations.

The surprisingly high incidence of atrial diverticula in patients with massive hydrocephalus could represent selection bias in assembling the cases for analysis. However, we believe, instead, that awareness of the phenomenon has led to careful examination of the incisura by serial 3–5 mm axial contrast-enhanced CT sections and to frequent use of direct coronal contrast-enhanced CT in these patients with consequent demonstration of changes previously overlooked.

To summarize, lateral ventricular diverticula may be distinguished from diverticula of the third ventricle, the ballooned fourth ventricle, and primary incisural arachnoid cysts by new CT criteria based firmly on the anatomic derangements peculiar to each group of lesions. It is to be expected, however, that strategically situated cysts and lucent solid masses may cause mass effects identical with those of the atrial diverticulum. Failure to appreciate the thin intervening wall could then lead to possible misdiagnosis of an atrial diverticulum on rare occasions.

ACKNOWLEDGMENTS

We thank Carol Fabian, Carol Wald, Olga Guzman, Arthur Nieves, Doree Shandera, Pat Sullivan, Carol Freda, Tracy Kolbas, Gloria Short, Gary Dettl, Andy Piper, and Angelo Mantas for help in manuscript preparation.

REFERENCES

1. Meese W, Lanksch W, Wende S. Diagnosis and postoperative follow-up studies of infantile hydrocephalus using computerized tomography. In: Lanksch W, Kazner E, eds. *Cranial computerized tomography*. Berlin: Springer, **1976**:424–429
2. Drayer BP, Rosenbaum AE, Maroon JC, Bank WO, Woodford JE. Posterior fossa extraaxial cyst: diagnosis with metrizamide CT cisternography. *AJR* **1977**;128:431–436
3. Fitz CR, Harwood-Nash DC, Chuang S, Resjo IM. Metrizamide ventriculography and computed tomography in infants and children. *Neuroradiology* **1978**;16:6–9
4. Marc JA, Khan A, Pillari G, Rosenthal A, Baron MG. Positive contrast ventriculography combined with computed tomography: technique and applications. *J Comput Assist Tomogr* **1980**;4:608–613
5. Sivalingam S, Dublin AB, Youmans JR. Computer assisted ventriculography. *J Comput Assist Tomogr* **1978**;2:162–164
6. Ruscalleda J, Guardia E, Fabio M dos Santos, Carvajal A. Dynamic study of arachnoid cysts with metrizamide. *Neuroradiology* **1980**;20:185–189
7. Roberts M, Hanaway J. *Atlas of the human brain in section*. Philadelphia: Lea & Febiger, **1971**
8. Childe AE, McNaughton FL. Diverticula of the lateral ventricles extending into the cerebellar fossa. *Arch Neurol Psychiatry* **1942**;47:768–778
9. Sweet WH. Spontaneous cerebral ventriculostium. *Arch Neurol Psychiatry* **1940**;44:532–540
10. MacFarlane WV, Falconer MA. Diverticulum of the lateral ventricle extending into the posterior cranial fossa: report of a case successfully relieved by operation. *J Neurol Neurosurg Psychiatry* **1947**;10:100–106
11. Russell DS. *Observations on the pathology of hydrocephalus*. Medical Research Council Special Report, series 265. London: His Majesty's Stationery Office, **1949**:124–128
12. Pennybacker J, Russell DS. Spontaneous ventricular rupture in hydrocephalus, with subtentorial cyst formation. *J Neurol Neurosurg Psychiatry* **1943**;6:38–45
13. Penfield W. Diencephalic autonomic epilepsy. *Arch Neurol Psychiatry* **1929**;22:358–374
14. Torkildsen A. Spontaneous rupture of the cerebral ventricles. *J Neurosurg* **1948**;5:327–339
15. Mott M, Cummins B. Hydrocephalus related to pulsion diverticulum of lateral ventricle. *Arch Dis Child* **1974**;48:407–410
16. Naidich TP, Pudlowski RM, Leeds NE, Naidich JB, Chisolm AJ, Rifkin MD. The normal contrast-enhanced computed axial tomogram of the brain. *J Comput Assist Tomogr* **1977**;1:16–19
17. Naidich TP, Leeds NE, Kricheff II, Pudlowski RM, Naidich JB, Zimmerman RD. The tentorium in axial section. I. Normal CT appearance and nonneoplastic pathology. *Radiology* **1977**;123:631–638
18. Naidich TP, Leeds NE, Kricheff II, Pudlowski RM, Naidich JB, Zimmerman RD. The tentorium in axial section. II. Lesion localization. *Radiology* **1977**;123:639–648
19. Ostertag CB, Mundinger F. Diagnosis of normal-pressure hydrocephalus using CT with CSF enhancement. *Neuroradiology* **1978**;16:216–219
20. Dyke CG. Acquired subtentorial pressure diverticulum of a cerebral lateral ventricle. *Radiology* **1942**;39:167–174
21. Zimmerman RA, Bilaniuk LT, Gallo E. Computed tomography of the trapped fourth ventricle. *AJR* **1978**;130:503–506
22. Scotti G, Musgrave MA, Fitz CR, Harwood-Nash DC. The isolated fourth ventricle in children: CT and clinical review of 16 cases. *AJNR* **1980**;1:419–424
23. Wolpert SM, Scott RM. The value of metrizamide CT cisternography in the management of cerebral arachnoid cysts. *AJNR* **1981**;2:29–35
24. Perryman CR, Pendergrass EP. Herniation of the cerebral ventricles. *AJR* **1948**;59:27–51
25. Kruyff E. Paracollicular plate cysts. *AJR* **1965**;95:899–916
26. Alonso A, Taboada D, Alvarez JA, Paramo C, Vila M. Spontaneous ventriculostomy and ventricular diverticulum. *Radiology* **1979**;133:651–654
27. Kapila A, Naidich TP. Spontaneous lateral ventriculocisternostomy documented by metrizamide CT ventriculography. *J Neurosurg* **1981**;54:101–104
28. Miller CF II, White RJ, Roski RA. Spontaneous ventriculocisternostomy. *Surg Neurol* **1979**;11:63–66
29. Mann KS, Khosla VK, Gulati DR. Congenital ventriculocisternostomy. *J Neurosurg* **1981**;54:98–100
30. Kanjilal GC. Spontaneous cerebral ventriculostium: two cases. *J Neurol Neurosurg Psychiatry* **1972**;35:676–681
31. Schechter MM, Rovit RL, Nelson K. Spontaneous "high pressure CSF rhinorrhoea"; cerebrospinal fluid leakage caused by longstanding increased intracranial pressure. *Br J Radiol* **1969**;42:619–622